

Flexible metal grating based optical fiber probe for photonic integrated circuits

Stijn Scheerlinck,^{a)} Dirk Taillaert, Dries Van Thourhout, and Roel Baets

Photonics Research Group, IMEC-Ghent University, Sint-Pietersnieuwstraat 41, 9000 Gent, Belgium

(Received 12 November 2007; accepted 3 December 2007; published online 23 January 2008)

An optical probe for photonic integrated circuits is proposed and demonstrated. The device is based on a single-mode fiber containing a subwavelength period metal grating on the facet. When approaching an integrated waveguide, light can be efficiently coupled between probe and waveguide without the need for integrated coupling structures, paving the way for wafer-scale circuit testing. A nanoimprint-and-transfer process were developed for fabricating this probe in a single step. We report 15% coupling efficiency between a gold grating fiber probe and a $220\text{ nm} \times 3\text{ }\mu\text{m}$ silicon-on-insulator waveguide and demonstrate testing of an integrated microring resonator using two probes. © 2008 American Institute of Physics. [DOI: 10.1063/1.2827589]

An important step toward widescale applications of photonic integrated circuits is the ability to test the operation and performance of circuit parts and components on a wafer scale. In microelectronics manufacturing, probes exist in the form of metal tips and are widely used for wafer-scale, non-destructive, and parametric testing.¹ An optical equivalent does not yet exist. As a result, testing of photonic integrated circuits requires either cleaving of facets for butt coupling or integration of grating couplers for normal incidence coupling,² both of which being permanent solutions and far from flexible. Probes based on modified fibers have been proposed. Angled-facet fibers,³ eroded fibers,⁴ and fiber tapers,⁵ placed parallel to the circuit plane allow testing of integrated components through evanescent coupling. However, coupling efficiency and bandwidth largely depend on the integration of phase-matching structures into the circuit,⁶ and the area needed for probing is in the order of at least several millimeters,⁵ making them unsuitable for highly integrated micro- and nanophotonic circuits. Optical fibers tapered down to extremely small tip sizes and placed normal to the circuit plane used for scanning near-field optical microscopy (SNOM) could also be applied for testing.⁷ However, the coupling efficiency between those fiber tips and integrated waveguides is very low.⁸ SNOM fiber tips are also difficult to fabricate⁹ and delicate in usage so that testing of integrated photonic circuits requires dedicated and costly SNOM-setup equipment.

In this paper, we propose a flexible and efficient optical fiber probe used in a normal incidence geometry with a probing area as small as the fiber diameter that does not need integrated coupling structures. The probe consists of a single-mode fiber with a strong diffraction grating on the core facet. This can be a metal grating or a dielectric grating that provides a sufficiently high refractive index contrast. The grating is designed such that broadband light is efficiently delivered to or captured from waveguides in the circuit. The main advantage of this probe is that it offers a high degree of flexibility. In particular, two probes provide a mechanism to verify whether light can flow between any two points in a circuit while at the same time, the spectral properties of the optical path established between those two

points can be addressed. A schematic of probing a highly integrated photonic circuit is depicted in Fig. 1(a). The two probes contain a subwavelength period metal grating and are brought within evanescent field distance to the waveguide [Fig. 1(b)]. The light guided by the top waveguide layer will be captured by the fiber, as is illustrated by the field plot in Fig. 1(c).

The proposed optical probe requires a subwavelength period metal grating pattern defined on an area as small as the core facet of a single-mode optical fiber and at a predetermined angle with respect to the fiber axis. This is rather challenging to fabricate. Direct-write approaches for subwavelength metal patterning on small substrates have been developed by several groups. They are based on focused ion beam milling¹⁰⁻¹³ or e-beam lithography.¹⁴ However, given the need for alignment and control of the angle between the grating plane and the fiber axis as will be explained further, these direct-write approaches require extra time-consuming processing steps. Nanoimprint lithography is a much more suitable technique and is capable of very high resolution patterning at low cost on a variety of substrate materials and shapes.¹⁵⁻¹⁷ In this paper, a UV-based nanoimprint and transfer technique is demonstrated for single step fabrication of the metal grating fiber probe.

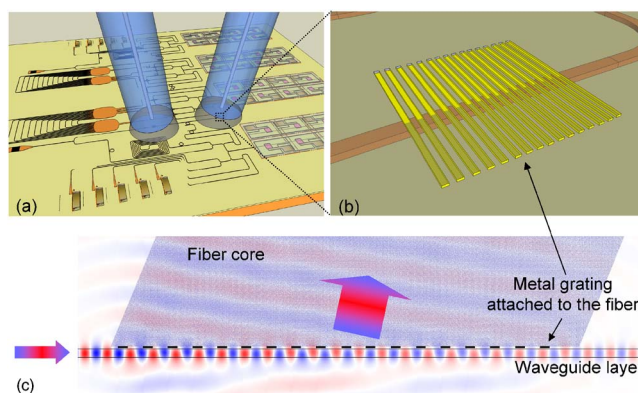


FIG. 1. (Color online) (a) Testing an integrated nanophotonic circuit using metal grating fiber probes. The orange arrows represent the flow of light. (b) Light is coupled between the fiber and the waveguide via metal grating attached to the fiber facet. (c) Two-dimensional field plot of metal grating induced light coupling between the waveguide and the fiber probe.

^{a)}Electronic mail: stijn.scheerlinck@intec.ugent.be.

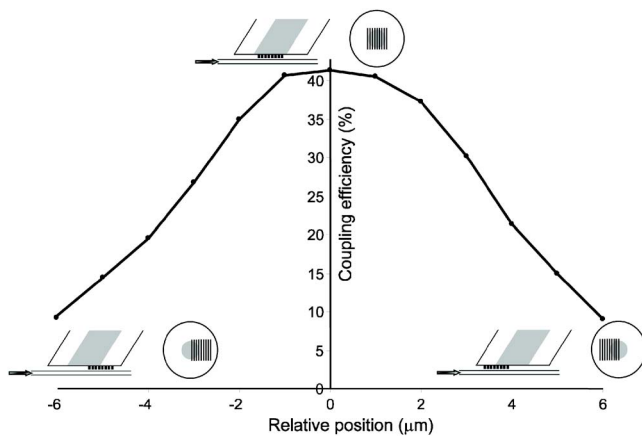


FIG. 2. (Color online) Alignment tolerancy analysis by two-dimensional FDTD calculations. The coupling efficiency is calculated as a function of relative position of the gold grating with respect to the fiber core. The insets illustrate the relative grating position.

We designed and fabricated gold grating fiber probes for silicon on insulator (SOI), a promising platform for nanophotonic circuits.^{18,19} In previous work, we demonstrated 34% coupling efficiency and a 1 dB bandwidth of 40 nm for TE polarization for a 630 nm period gold grating on top of a $10\ \mu\text{m} \times 220\ \text{nm}$ silicon waveguide.²⁰ Coupling is optimal when the phase fronts make an angle of 10° with respect to the vertical. This result is taken as the starting point of the fiber probe design fixing the angle between the grating plane and the fiber axis to 80° . Although vertical coupling can be achieved by a smaller grating period, the angled configuration is necessary to avoid large secondary order reflections back into the circuit that might lead to cavity formation, instability, and deterioration of the performance of integrated components.

The optimal position of the gold grating with respect to the core was investigated by two-dimensional finite difference time domain (FDTD) calculations (OMNISM 4.0, PhotonDesign). In the simulations, the single-mode fiber consists of a 1.46 refractive index core surrounded by a 1.455 refractive index cladding. The probe grating is assumed in contact with the waveguide. The coupling efficiency at a wavelength of 1540 nm as a function of relative grating position with respect to the fiber core is plotted in Fig. 2. It follows that alignment to the fiber core within a tolerancy frame of a few microns is necessary for sufficient coupling, illustrating the importance of alignment for the performance of the fiber probe. It also follows that a grating, which is too large compared to the core diameter, has limited or no coupling efficiency as light will be coupled out without being captured by the fiber core.

Probing with the gold grating fiber probe requires that the distance between the top of the waveguide and the gold grating is within the evanescent field decay length of the waveguide mode. FDTD calculations show a drop in coupling efficiency from 40% to less than 4% when the distance to the waveguide exceeds 200 nm.

The fabrication process flow is depicted in Fig. 3. Starting point of the process is a standard straight-cleaved single-mode fiber and a specially prepared SOI mold carrying the gold pattern that is to be transferred to the fiber facet. The mold was obtained in the following way. First, the SOI sample containing $10 \times 10\ \mu\text{m}^2$ gratings of period 630 nm

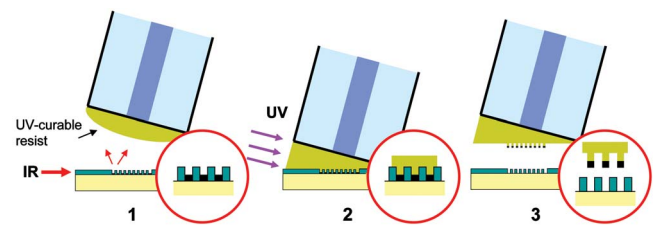


FIG. 3. (Color online) Fiber probe fabrication using nanoimprint and transfer lithography. First, the fiber with UV-curable resist is aligned over the specially prepared mold carrying the $10 \times 10\ \mu\text{m}^2$ gold grating pattern in the mold trenches. Then, the cavities are filled and the resist is UV cured. Finally, the mold is released. The metal grating is now attached to the fiber.

and an etch depth of 220 nm was treated with an antistiction coating. Then, gold was evaporated onto the mold. Finally, the gold on top of the mold grating lines was selectively removed by microcontact printing on another substrate. In this way, the original SOI mold becomes a carrier of the gold grating pattern by leaving the gold only in the grating trenches.

For probe fabrication, the mold was fixed on a vacuum chuck and the fiber was mounted on a x, y, z stage and tilted at a 10° angle with respect to the normal of the mold. Then, the fiber was dipped in a drop of UV-curable resist. We used PAK-01 (Toyo Gosei, Co.). First, the fiber was passively aligned using a microscope. Then, the fiber was connected to a photodetector and the light from a broadband source with central wavelength of 1535 nm was sent into the top waveguide layer of the mold. The light scattered out by the grating was used to align the fiber core to the grating actively. This is illustrated in Fig. 3. When the fiber was brought closer to the mold, the resist was allowed to fill the grating trench cavities in the mold as is the case in a conventional nanoimprint process using low-viscous resist. The resist was then cured by UV light (EFOS Ultracure 100ss-plus) and the fiber was lifted from the mold. The strong adhesion between the polymer and the gold pattern as opposed to the low adhesion between the gold and the silica and between the polymer and the pretreated silicon caused a transfer of the gold grating pattern from the mold to the fiber facet. The whole process was carried out at room temperature. In this way, gold grating fiber probes were fabricated that are very robust and could be used in multiple experiments in a standard measurement setup. Figure 4 depicts microscope and scanning electron microscopy (SEM) images of the fiber probe facet. The pictures were taken after the experiments described below.

The coupling efficiency was experimentally determined. Two gold grating fiber probes were fabricated, both consisting of a gold grating of thickness 20 nm and grating period of 630 nm. Both probes were brought into contact with a

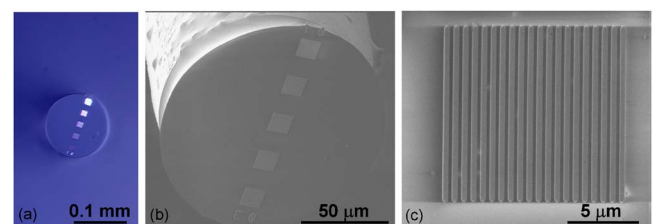


FIG. 4. (Color online) (a) Microscope image of the fiber probe facet containing $10 \times 10\ \mu\text{m}^2$ gold gratings. (b) SEM picture of the fiber facet. The middle grating is aligned to the core. (c) Detail of the gold grating.

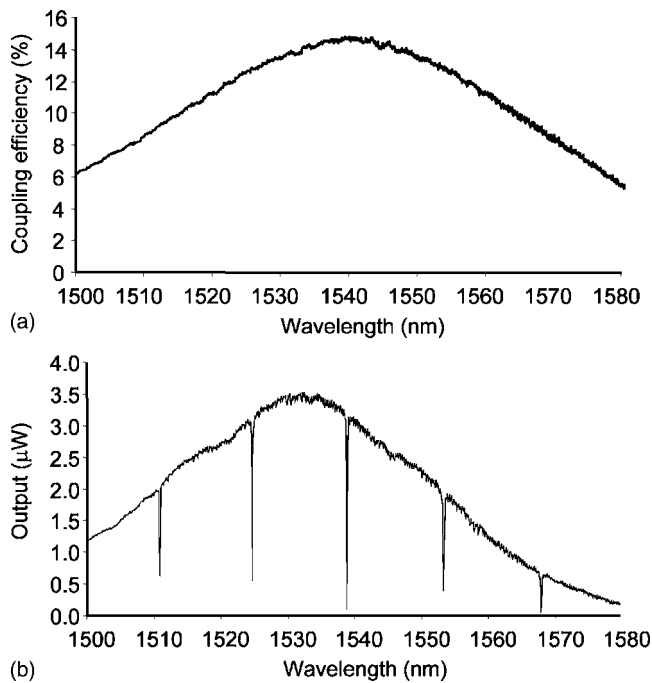


FIG. 5. (a) Experimentally determined wavelength-dependent coupling efficiency between a gold fiber probe and a $220\text{ nm} \times 3\text{ }\mu\text{m}$ waveguide. (b) Testing of a SOI microring resonator using two probes.

straight $220\text{ nm} \times 3\text{ }\mu\text{m}$ SOI waveguide using a standard setup for normal incidence fiber-to-waveguide coupling. One probe was then connected to a tunable laser source with an output power of 1 mW. The other was connected to a photodetector. Polarization wheels were used to control polarization. Assuming identical probes and a lossless waveguide, 15% coupling efficiency could be demonstrated at a wavelength of 1545 nm with a 1 dB bandwidth of 38 nm. The result is plotted in Fig. 5(a).

As a demonstration, two gold grating fiber probes were applied to test an integrated SOI microring resonator with photonic wire dimensions of $220 \times 500\text{ nm}^2$. In particular, the first probe was used to deliver light to the $220\text{ nm} \times 3\text{ }\mu\text{m}$ input waveguide and the second probe was used to capture the light from the $220\text{ nm} \times 3\text{ }\mu\text{m}$ output waveguide. We obtained the pass spectrum depicted in Fig. 5(b). As expected, the output drops drastically at resonant wavelengths of the ring resonator. These data can be used for further analysis of the performance of the microring resonator such as Q factor, finesse, round trip loss, etc.

In conclusion, a metal grating fiber probe for probing and testing integrated photonic circuits was proposed. The device consists of a metal diffraction grating at an angled facet aligned to the fiber core. Gold grating fiber probes were fabricated and demonstrated 15% coupling efficiency to SOI

waveguides and a 1 dB bandwidth of 38 nm. The pass spectrum of a SOI integrated microring resonator was successfully measured. An UV-based nanoimprint and transfer process was developed to fabricate gold grating fiber probes. This process can be useful in a broad range of applications where metal nanopatterns are needed on small substrates. The demonstrated metal grating fiber probe is a potential candidate for low-cost and wafer-scale testing of highly integrated nanophotonic circuits.

This work was partly supported by the European Union through IST-ePIXnet and the Silicon Photonics Platform, by the Belgian (IAP)-PHOTON and the IAP-Photonics@be project, and by Ghent University through the GOA biosensor project. S. Scheerlinck thanks the Institute for the Promotion of Innovation through Science and Technology in Flanders (IWT-Vlaanderen) for a scholarship.

- ¹D. Gizopoulos, *Advances in Electronic Testing: Challenges and Methodologies* (Springer, Dordrecht, 2006), Vol. 27, p. 1.
- ²D. Taillaert, F. Van Laere, M. Ayre, W. Bogaerts, D. Van Thourhout, P. Bienstman, and R. Baets, *Jpn. J. Appl. Phys., Part 1*, **45**, 6071 (2006).
- ³V. S. Ilchenko, X. S. Yao, and L. Maleki, *Opt. Lett.* **24**, 723 (1999).
- ⁴N. Dubreuil, J. C. Knight, D. K. Leventhal, V. Sandoghdar, J. Hare, and V. Lefevre, *Opt. Lett.* **20**, 813 (1995).
- ⁵C. P. Michael, M. Borselli, T. J. Johnson, C. Chrystal, and O. Painter, *Opt. Express* **15**, 4745 (2007).
- ⁶P. E. Barclay, K. Srinivasan, M. Borselli, and O. Painter, *Appl. Phys. Lett.* **85**, 4 (2004).
- ⁷S. Bourzeix, J. M. Moison, F. Mignard, F. Barthe, A. C. Boccara, C. Licoppe, B. Mersali, M. Allovon, and A. Bruno, *Appl. Phys. Lett.* **73**, 1035 (1998).
- ⁸J. T. Robinson, S. F. Preble, and M. Lipson, *Opt. Express* **14**, 10588 (2006).
- ⁹N. Chevalier, Y. Sonnefraud, J. F. Motte, S. Huant, and K. Karrai, *Rev. Sci. Instrum.* **77**, 063704 (2006).
- ¹⁰A. Partovi, D. Peale, M. Wuttig, C. A. Murray, G. Zydzik, L. Hopkins, K. Baldwin, W. S. Hobson, J. Wynn, J. Lopata, L. Dhar, R. Chichester, and J. H. Yeh, *Appl. Phys. Lett.* **75**, 1515 (1999).
- ¹¹F. Chen, A. Itagi, J. A. Bain, D. D. Stancil, T. E. Schlesinger, L. Stebounova, G. C. Walker, and B. B. Akhremitchev, *Appl. Phys. Lett.* **83**, 3245 (2003).
- ¹²E. Cubukcu, E. A. Kort, K. B. Crozier, and F. Capasso, *Appl. Phys. Lett.* **89**, 093120 (2006).
- ¹³E. J. Smythe, E. Cubukcu, and F. Capasso, *Opt. Express* **15**, 7439 (2007).
- ¹⁴P. S. Kelkar, J. Beauvais, E. Lavallee, D. Drouin, M. Cloutier, D. Turcotte, P. Yang, L. K. Mun, R. Legario, Y. Awad, and V. Aimez, *J. Vac. Sci. Technol. A* **22**, 743 (2004).
- ¹⁵S. Y. Chou, P. R. Krauss, and P. J. Renstrom, *J. Vac. Sci. Technol. B* **14**, 4129 (1996).
- ¹⁶L. J. Guo, *Adv. Mater. (Weinheim, Ger.)* **19**, 495 (2007).
- ¹⁷J. Viheriala, T. Niemi, J. Kontio, T. Ryttonen, and M. Pessa, *Electron. Lett.* **43**, 150 (2007).
- ¹⁸W. Bogaerts, R. Baets, P. Dumon, V. Wiaux, S. Beckx, D. Taillaert, B. Luyssaert, J. Van Campenhout, P. Bienstman, and D. Van Thourhout, *J. Lightwave Technol.* **23**, 401 (2005).
- ¹⁹R. Soref, *IEEE J. Sel. Top. Quantum Electron.* **12**, 1678 (2006).
- ²⁰S. Scheerlinck, J. Schrauwen, F. Van Laere, D. Taillaert, D. Van Thourhout, and R. Baets, *Opt. Express* **15**, 9639 (2007).